JOURNAL OF SPACECRAFT AND ROCKETS
Vol. 32, No. 6, November–December 1995

Designing Continuous-Thrust Low-Earth-Orbit to Geosynchronous-Earth-Orbit Transfers

David B. Spencer*
Phillips Laboratory, Kirtland Air Force Base, New Mexico 87117-5776
and
Robert D. Culp†
University of Colorado, Boulder, Colorado 80309-0429

This paper examines a method that can be used to transfer a spacecraft from a circular low Earth orbit (LEO), inclined to the equator, to a circular geosynchronous Earth orbit (GEO) with no inclination. The principle is to minimize the propulsive-mass cost for a continuously thrusting vehicle with the capability for multiple on–off thrusting cycles. The analysis was conducted for a large range of initial accelerations, and it was found that the method is best used to bridge the gap between very low-thrust transfers and high-thrust, impulsive transfers. The simulation of a LEO–GEO transfer showed that the results varied from 1% over the optimal cost for a high-thrust transfer, to 2.5% over the optimal cost for an intermediate-thrust transfer, to 0.3% over the cost of a low-thrust, spiral transfer. This makes this technique a good first estimate algorithm for the entire range of high- to low-thrust transfers.

Nomenclature

a	= semimajor axis of orbit, km
c	= thruster exhaust velocity, m/s
E	= specific energy, m^2/s^2
e	= eccentricity of orbit
g_0	= acceleration at sea level, m/s^2
h	= first equinoctial element relating eccentricity, node, and argument of perigee
I_{sp}	= specific impulse, s
i	= inclination of orbit, rad
k	= second equinoctial element relating eccentricity, node, and argument of perigee
$\mathbf{M}$	= 6×3 matrix mapping thrust vector to differential equations
M	= mean anomaly, rad
$m(t)$	= mass of spacecraft at time t
m_i	= mass of spacecraft after ith burn
n	= mean motion of orbit, rad/s
p	= first equinoctial element relating inclination and node
q	= second equinoctial element relating inclination and node
r, r_a, r_p	= instantaneous, apogee, and perigee radius, km
T/m_0	= initial thrust-to-mass ratio, N/kg (also m/s^2)
t_0	= initial time
t_f	= final time
$\boldsymbol{X}$	= state vector, $(a\ h\ k\ p\ q\ \lambda)^T$
$\hat{\boldsymbol{u}}$	= $(u_f\ u_g\ u_w)^T$ three-element control vector
v, v_a, v_p	= instantaneous, apogee, and perigee velocity, m/s
α, β	= pitch and yaw control angle, rad
Δv	= effective velocity change, m/s
$\Delta v_i,\ i = 1, 2$	= Hohmann-transfer velocity change, m/s
δ	= $\begin{cases} 1 & \text{during burn arc} \\ 0 & \text{during coast arc} \end{cases}$
ζ	= $(0\ 0\ 0\ 0\ 0\ 1)^T$
$\eta(t)$	= mass ratio at time t
λ	= mean longitude, rad
μ	= gravitational parameter, 398,600.8 km^3/s^2
τ	= total burn-arc time duration, seconds
Ω	= right ascension of ascending node, rad
ω	= argument of perigee, rad

Received June 6, 1994; revision received Nov. 22, 1994; accepted for publication Dec. 2, 1994. This paper is declared a work of the U.S. Government and is not subject to copyright protection in the United States.

*Orbital Dynamics Program Manager, Space and Missiles Dynamics Division, 3550 Aberdeen Avenue.

†Professor and Chairman, Department of Aerospace Engineering Sciences, Campus Box 429.

Introduction

THE complexities of performing a transfer between a low Earth orbit (LEO) and a geosynchronous Earth orbit (GEO) are such that an analytical study is difficult to accomplish. Simplifications and approximations that are acceptable for some types of problems are limited by the assumptions made. Analytical approximations work for many cases, such as very low thrust, where a spiral approximation can match accurately what truly happens. Likewise, impulsive approximations (infinite thrust, infinitely small duration) can also yield valid results. In between, for intermediate-level thrust, neither spiral approximations nor infinitely-small-thrust-duration approximations are valid.

The problem to be examined in the course of this paper will be that of determining an approximate orbit transfer cost for a continuously thrusting propulsion system (with multiple on–off switching) and comparing it with the optimal orbit transfer cost. Short of a numerical optimization process, there is no simple way to determine the best way to perform a three-dimensional transfer where the orbit plane is changing at the same time as the shape of the planar orbit. However, some simplifications and assumptions can be made to allow for an easier solution procedure. Additionally, a variation of the thrust-to-mass ratios was studied, and the effects of this parameter on the mass cost were determined.

In the design phase, sizing of the system occurs, and the value of having a simple method to determine the near-optimal cost is very important. The methods presented here are further detailed in Refs. 1–3.

Analysis

In this section, the natural dynamical equations of motion in an inverse-square gravitational field, with a perturbation vector in the form of a propulsive force, are presented. Next, several control laws are developed, each with a specific goal in mind, on the way to completing the three-dimensional LEO–GEO transfer.

Several element sets were considered for use in this analysis. Earth-centered inertial (ECI) elements $(x, y, z, \dot{x}, \dot{y}, \dot{z})$ are easily implemented, but show little insight into the behavior of the system.

Classical elements $(a, e, i, \Omega, \omega, M)$ give good physical insight into the system, but prove difficult for low-eccentricity and low-inclination orbits. Equinoctial elements[4] eliminate several of the singularities of the classical elements and prove useful for the specific cases to be studied. Because of this, the equinoctial orbital elements are used for the analysis throughout the course of this paper, with the occasional use of classical elements to provide physical insight.

The equations of motion are presented in matrix form, as

$$\frac{dX}{dt} = \frac{T\delta}{m(t)}M\hat{u} + n\zeta \tag{1}$$

and the mass flow equation is

$$\frac{dm(t)}{dt} = -\frac{T\delta}{c} \tag{2}$$

The elements of the matrix $\mathbf{M}$ are derived in Ref. 5, among others, and are shown in the Appendix. To eliminate the need for a value of the mass, Eq. (2) is nondimensionalized by introducing the variable

$$\eta(t) = \frac{m(t)}{m_0} \tag{3}$$

with the time derivative of η being

$$\frac{d\eta}{dt} = \frac{\delta}{m_0}\frac{dm}{dt} = -\frac{T\delta}{m_0}\frac{1}{c} \tag{4}$$

The ratio $T/m(t)$ is replaced in Eq. (1) by $(T/m_0)(1/\eta(t))$. This then gives seven differential equations to be solved.

First Burn Arc in LEO–GEO Transfer: Maximization of da/dt Control Law

If there are no attitude constraints, a simple control law where the amount of energy put into the system is maximized can be used. The energy is found from the simple relation

$$E = -\frac{\mu}{2a} \tag{5}$$

Taking the time derivative of Eq. (5), we get

$$\frac{dE}{dt} = \frac{\mu}{2a^2}\frac{da}{dt} \tag{6}$$

Thus, maximizing the time rate of change of energy is equivalent to maximizing the time rate of change of semimajor axis.

If the pitch angle of the transfer is designated by the angle α, and the yaw angle is designated by the angle β, the control variables u_f, u_g, and u_w in the equinoctial reference frame, become

$$u_f = \cos\alpha\cos\beta \tag{7}$$

$$u_g = \sin\alpha\cos\beta \tag{8}$$

$$u_w = \sin\beta \tag{9}$$

Expanding the first row of Eq. (1) (with the nondimensional transformation of mass), and noting that $M_{13} = 0$ (Ref. 5), we have

$$\frac{da}{dt} = \frac{T\delta}{m_0}\frac{1}{\eta(t)}(M_{11}\cos\alpha\cos\beta + M_{12}\sin\alpha\cos\beta) \tag{10}$$

Taking the partial derivative of Eq. (10) with respect to the control angle α, assuming that $\cos\beta$ is not equal to zero, and setting the partial derivative equal to zero maximizes the time rate of change in the semimajor axis a [since the minimum value of Eq. (10) is negative, which means that the semimajor axis is decreasing, which is the opposite of the desired goal]. Doing this, the control law becomes

$$\alpha = \tan^{-1}\left(\frac{M_{12}}{M_{11}}\right) \tag{11}$$

For many cases, it is not cost-effective to have only one burn arc for the transfer. In these cases, a coast arc is inserted between two burn arcs. The point where the coast arc begins is determined from the integration using the control law for the first burn. When the apogee radius found from the integration reaches the apogee radius desired, the thrust is turned off.

Plane Change Maneuver in a LEO–GEO Transfer Orbit

As the spacecraft is approaching its first apogee pass of the coast arc, the second maneuver begins. This maneuver is the plane change maneuver. When the spacecraft is moving the slowest, then application of a plane change maneuver is most efficient. That is why it is done secondly. In the impulsive case, a plane change and a recircularization maneuver are combined, but for this study, they are examined independently. The assumption here is that because of the finite-duration burn arc (as opposed to an impulsive burn), the plane change is spread throughout the apogee passage. Additionally, the apogee passage is designed to coincide with the nodal crossing, to allow for a final equatorial orbit. The goal is to perform half of the maneuver before the apogee is reached, and the other half after the apogee passage. In this simulation, the out-of-plane maneuver was designed to take place in a similar length of time to what it takes to recircularize the final orbit. This becomes an iterative process, but proved to be a workable solution.

The determination of the thrust vector is now addressed. Just as the pitch angle α controls the eccentricity, the yaw angle β controls the inclination. The relationship between the inclination and the equinoctial elements, p and q, is

$$i = 2\tan^{-1}(p^2 + q^2)^{\frac{1}{2}} \tag{12}$$

Taking the derivative of this equation with respect to time yields

$$\frac{di}{dt} = \frac{2(p\dot{p} + q\dot{q})}{(p^2 + q^2)^{\frac{1}{2}}(1 + p^2 + q^2)} \tag{13}$$

Since the variables p and q are influenced by a change in the yaw angle β, the inclination time history does not depend on the yaw angle directly. This is shown by inserting the values of the differential equations from Eq. (1), as well as the control-angle definitions, into Eq. (13), which simplifies to

$$\frac{di}{dt} = \frac{2(pM_{43} + qM_{53})}{(p^2 + q^2)^{\frac{1}{2}}(1 + p^2 + q^2)}\sin\beta \tag{14}$$

To determine the value of β that maximizes Eq. (14), take the partial derivative with respect to the angle β. Then setting that to result to zero yields

$$\cos\beta = 0 \tag{15}$$

Thus

$$\beta = \pm 90\,\text{deg} \tag{16}$$

To determine whether this is a maximum or minimum, and when to use the positive or negative sign, the second-derivative test yields the condition that

$$(pM_{43} + qM_{53})\sin\beta > 0 \tag{17}$$

Checking the sign of $pM_{43} + qM_{53}$ determines whether to use the positive or negative value found for β. The plane change maneuver ends when the desired inclination is reached.

Recircularizing the Transfer Orbit

The last step in reaching a GEO is to recircularize the orbit. Here, the goal is to change the perigee radius, while keeping the apogee radius constant. This can be done by examining the dynamics of the perigee radius. Since this is a coplanar maneuver, the angle $\beta = 0$. The radius at perigee is found as

$$r_p = a(1 - e) \tag{18}$$

The time rate of change in perigee radius is

$$\frac{dr_p}{dt} = -a\frac{de}{dt} + \frac{da}{dt}(1-e) \tag{19}$$

In addition to changing the perigee radius, the apogee radius must remain constant. With the apogee radius given as

$$r_a = a(1+e) \tag{20}$$

and the time derivative set equal to zero,

$$\frac{dr_a}{dt} = 0 = a\frac{de}{dt} + (1+e)\frac{da}{dt} \tag{21}$$

the time derivative of the semimajor axis can be solved for

$$\frac{da}{dt} = -\frac{a}{1+e}\frac{de}{dt} \tag{22}$$

The eccentricity is related to the equinoctial elements by

$$e = (h^2 + k^2)^{\frac{1}{2}} \tag{23}$$

Taking the time derivative of Eq. (22) yields

$$\frac{de}{dt} = \frac{1}{(h^2+k^2)^{\frac{1}{2}}}(h\dot{h} + k\dot{k}) \tag{24}$$

Inserting Eq. (24) into Eq. (19), the time derivative of perigee radius with constant apogee radius is

$$\frac{dr_p}{dt} = -\frac{2a}{1+e}\frac{de}{dt} = -\frac{2a}{(h^2+k^2)^{\frac{1}{2}} + h^2 + k^2}\left(h\frac{dh}{dt} + k\frac{dk}{dt}\right) \tag{25}$$

To obtain the control angle that maximizes the rate of change in perigee radius and keeps the apogee radius constant, take the partial derivative of Eq. (25) with respect to the control angle α, and set it equal zero. That control angle becomes

$$\alpha = \tan^{-1}\left\{\frac{\mp\left(hM_{21} + kM_{31} + \dfrac{e+e^2}{a}M_{11}\right)}{\pm\left(hM_{22} + kM_{32} + \dfrac{e+e^2}{a}M_{12}\right)}\right\} \tag{26}$$

To determine whether to use the positive or negative value of α, the second-derivative test on Eq. (26) shows that, to increase the perigee while keeping the apogee constant, the constraint

$$\frac{1}{\cos\alpha}(hM_{21} + kM_{31}) > 0 \tag{27}$$

must be satisfied.

When the position in the burn arc approaches the perigee radius, the perigee radius cannot be changed without increasing the apogee radius. Therefore, if the ratio of the instantaneous radius to the perigee radius is less than some threshold, say perhaps 1.01, the thrust is turned off, and a coast arc is instituted. This allows for a reasonable transfer time that does not waste propellant trying to increase the perigee radius when the spacecraft is at perigee. This situation occurs only when there are multiple perigee passes, which correspond to the lower-acceleration simulations.

Quality of the Solution

To study the quality of solutions obtained from the simulations, a metric must be used. For the high-thrust, coplanar transfer, the *best* case (the one that requires the lowest amount of propellant) is the two-impulse Hohmann transfer. The impulsive change in velocity for the first burn is computed from the well-known equation

$$\Delta v_1 = \left(\frac{\mu}{r_p}\right)^{\frac{1}{2}}\left\{\left[\frac{2(r_a/r_p)}{1+(r_a/r_p)}\right]^{\frac{1}{2}} - 1\right\} \tag{28}$$

while the impulsive change in velocity for the second burn is

$$\Delta v_2 = \left(\frac{\mu}{r_a}\right)^{\frac{1}{2}}\left\{1 - \left[\frac{2}{1+(r_a/r_p)}\right]^{\frac{1}{2}}\right\} \tag{29}$$

The amount of mass used is

$$\Delta m_i = m_{i-1}\left[1 - \exp\left(-\frac{\Delta v_i}{g_0 I_{sp}}\right)\right], \qquad i = 1, 2 \tag{30}$$

Converting to the nondimensional mass parameter, Eq. (30) becomes

$$\eta(t_i) = \eta(t_{i-1})\exp\left(-\frac{\Delta v_i}{g_0 I_{sp}}\right) \tag{31}$$

For an impulsive inclination change maneuver, the Δv requirement is

$$\Delta v = 2v\sin\frac{\Delta i}{2} \tag{32}$$

and to determine the associated mass or mass-parameter costs, Eq. (30) or (31) can again be used.

For a low-thrust, coplanar transfer, the approximate cost of the transfer is simply the difference in velocity between the perigee velocity and the apogee velocity,

$$\Delta v = v_p - v_a = v_p\left[1 - \left(\frac{r_p}{r_a}\right)^{\frac{1}{2}}\right] \tag{33}$$

The mass cost calculated is the solution of Eq. (2), which is a function of the specific impulse used. However, to eliminate the dependence on specific impulse, the cost can be changed into an "effective Δv." Integrating the mass-ratio rate (2) for N burn arcs yields

$$\sum_{i=0}^{N}\eta(t_{i+1}) - \eta(t_i) = -\frac{T}{m_0}\frac{1}{g_0 I_{sp}}\sum_{i=0}^{N}\delta(t_{i+1} - t_i) \tag{34}$$

The mass ratio changes only during the burn arc, so Eq. (34) reduces to

$$\eta(t_f) - \eta(t_0) = -\frac{T}{M_0}\frac{1}{g_0 I_{sp}}\tau. \tag{35}$$

Solving Eq. (31) for the sum total of burn arcs and the specific-impulse term yields

$$\frac{1}{g_0 I_{sp}} = -\frac{\ln\eta(t_f) - \ln\eta(t_0)}{\Delta v} \tag{36}$$

Inserting Eq. (36) into Eq. (35) and solving for the effective Δv gives

$$\Delta v = \frac{T}{m_0}\left[\frac{\ln\eta(t_f) - \ln\eta(t_0)}{\eta(t_f) - \eta(t_0)}\tau\right] \tag{37}$$

There have been various results published that give the "optimal" transfer parameters for a wide range of initial thrust-to-mass ratios. Each optimal case published has its own merits and limitations, and therefore none are used to gauge the results presented in this paper. The Hohmann-transfer approximation is still the best metric to judge the quality of the results for the high-thrust cases, and the velocity-difference method provides a good metric for the low-thrust cases. However, in between, there are very few results published that provide a metric for the intermediate-thrust cases.

Results

In this section, the transfers analyzed use initial thrust-to-mass ratios ranging from very high (100,000 N/kg) to very low (0.01 N/kg). Each transfer is a combination of orbit shape change and orbit plane change. Although simulations were performed for each initial thrust-to-mass ratio, in factors of 10, detailed results are presented only for one case, that being an initial thrust-to-mass ratio of 1.0 N/kg. This is a representative result of the intermediate-thrust regime. Further examples can be found in Ref. 2.

The simulation begins with a circular orbit, with a radius of 7000 km, inclined to the orbit at 28.5 deg, and ends with a circular orbit with a radius of approximately 42,241 km, with zero inclination. For numerical approximations, the initial eccentricity is set at an arbitary small value, as are the final eccentricity and inclination. The locations of the spacecraft in the initial and final orbits are artibrary and are coupled; they are therefore not presented, except that the initial mean anomaly is chosen so that the first burn arc ends at an equatorial crossing.

The cases presented here have three major burn arcs (the second and third burn arcs are sequential, and are effectively one burn arc), and possibly some smaller burn arcs in the recircularization maneuver (due to the multiple perigee passages for the very low-thrust cases, as previously discussed). In actual operations, the plane change and recircularization burns can be combined into one maneuver. This would reduce the impulsive cost by as much as 600 m/s and would likewise decrease the effective Δv for all of the transfers presented here.

All of the small burn arcs in the recircularization are included in the effective Δv for the recircularization. Table 1 shows the costs for this simulation for seven orders of magnitude in initial thrust-to-mass ratio, as well as the three-dimensional impulsive approximation and the two-dimensional spiral approximation.

For the coplanar spiral transfer, using the initial and final orbital altitudes, the difference between the velocity at perigee and the velocity at apogee is approximately 4475 m/s, which is 15 m/s greater than the sum of the cost of the first burn and recircularization burn(s) for the lowest initial thrust-to-mass ratio.

In Refs. 6 and 7 results were presented on optimal LEO–GEO transfers. Since the initial conditions are not the same in the two references and this study, the transfer costs are normalized with respect to the impulsive costs calculated in each study, and are presented in Fig. 1.

Next, a set of representative results are presented. This example case is for an initial thrust-to-mass ratio of 1 N/kg. The time histories for the classical orbital elements and the control angles for a typical intermediate-thrust simulation are shown in Figs. 2–6. The boldface lines represent burn arcs, and the thin lines represent coast arcs. The semimajor-axis time history of the transfer is presented in Fig. 2. The duration of the first burn arc is 2239 s, followed by a coast arc of 18,120 s. The plane change maneuver takes 630 s, and the transfer is completed with a recircularization maneuver of 888 s. Figure 3 shows the eccentricity time history. Notice the nearly linear growth and decay in eccentricity during the first burn arc and in the recircularization. For higher initial thrust-to-mass ratios, the slope on the eccentricity gets larger, and for the impulsive case, the slope becomes infinite. As the initial thrust-to-mass ratio decreases, the eccentricity time history shows a periodic variation, with a period of approximately one orbital revolution, and a much smaller amplitude. For the limiting case of a spiral, the eccentricity remains nearly equal to zero. Figure 4 shows the inclination time history. As with the eccentricity, the slope of the inclination change approaches infinity with increasing initial thrust-to-mass ratios, and decreases as the initial thrust-to-mass ratio decreases. Figure 5 shows the time histories of the apogee, perigee, and instantaneous radius during the transfer. Lastly, Fig. 6 shows the control-angle time histories. In this simulation, the in-plane control angle α changes during the in-plane

Table 1 Three-dimensional LEO–GEO transfer cost

T/m_0, N/kg	Effective Δv for first, burn m/s	Effective Δv for plane change burn, m/s	Effective Δv for recircularization, m/s	Total effective Δv, m/s
100,000	2338	810	1420	4568
10,000	2339	811	1419	4569
1,000	2339	814	1419	4572
100	2339	817	1419	4575
10	2341	819	1418	4578
1	2543	853	1352	4748
0.1	3785	1237	856	5878
0.01	4307	4549	153	9009
Three-impulse approx.	2338	805	1425	4568
Two-dimensional spiral approx.	N/A	N/A	N/A	4475

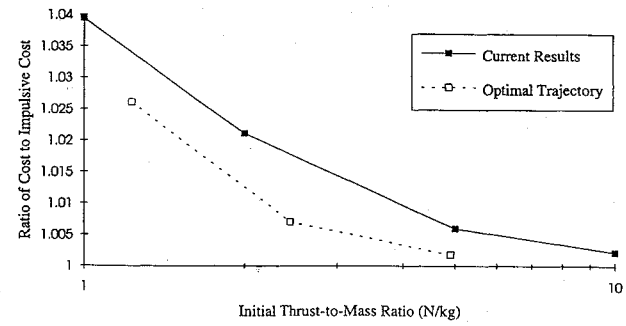

Fig. 1 Comparison of current study results to those of Refs. 6 and 7.

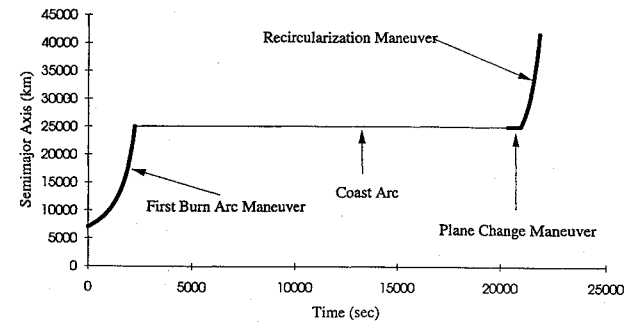

Fig. 2 Semimajor axis time history.

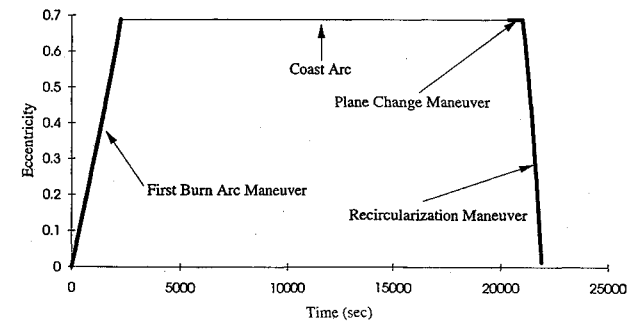

Fig. 3 Eccentricity time history.

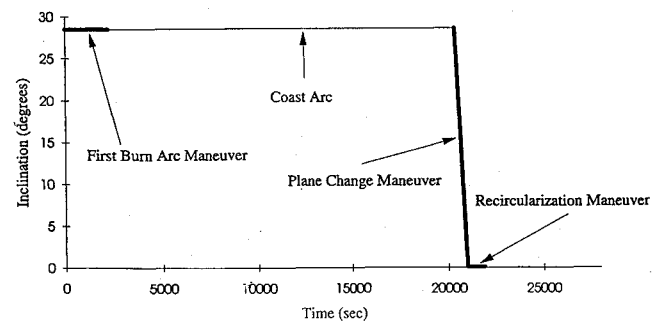

Fig. 4 Inclination time history.

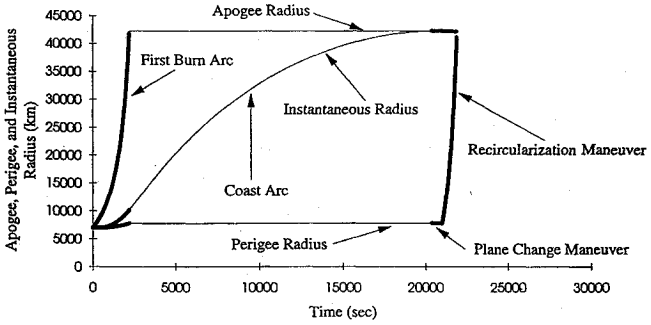

Fig. 5 Instantaneous radius, apogee radius, and perigee radius time histories.

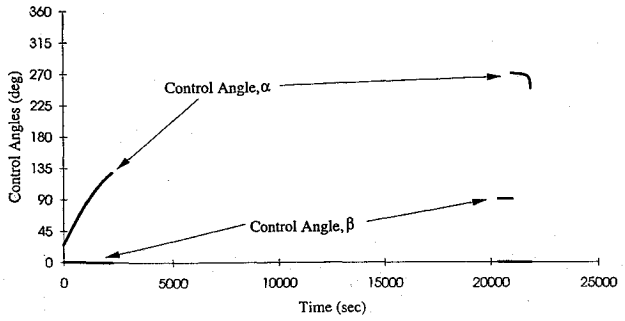

Fig. 6 Control angles α and β time histories.

maneuvers, while the yaw angle β is always equal to zero, except during the plane change maneuver, when it is equal to 90 deg. Further discussion of the time histories of the other cases presented in Table 1 can be found in Ref. 2.

Conclusions

This paper outlines a methodology to relax the requirement of an extensive numerical analysis of the optimal orbit transfer trajectory analysis. Simple yet physically realizable control laws were developed and applied to a number of initial thrust-to-mass ratios. The methodology presented here is not intended as a replacement for an optimization study, but as a complement to the numerical approach. It is best used for an initial design analysis, and for spacecraft onboard guidance systems.

The most significant result shown is that this method is applicable to a 7-order-of-magnitude range in initial thrust-to-mass ratios, which covers the spectrum of all orbit transfers, and can accurately model the region between high-thrust, impulsive approximations and low-thrust, spiral approximations.

Appendix: Matrix Elements

The constituents of the matrix in Eq. (1) are reprinted from Refs. 2 and 5. The additional variables are not included in the Nomenclature, since many are dummy variables and have no physical meaning. The elements of the matrix **M** are

$$M_{11} = \frac{2a}{nr}[hkb\cos F - (1-h^2b)\sin F] \tag{A1}$$

$$M_{12} = \frac{2a}{nr}[(1-k^2b)\cos F - hkb\sin F] \tag{A2}$$

$$M_{13} = 0 \tag{A3}$$

$$M_{21} = \frac{G}{na^2}\left(\frac{\partial X}{\partial k} - hb\frac{\dot{X}}{n}\right) \tag{A4}$$

$$M_{22} = \frac{G}{na^2}\left(\frac{\partial Y}{\partial k} - hb\frac{\dot{Y}}{n}\right) \tag{A5}$$

$$M_{23} = \frac{k}{Gna^2}(qY - qX) \tag{A6}$$

$$M_{31} = -\frac{G}{na^2}\left(\frac{\partial X}{\partial h} + kb\frac{\dot{X}}{n}\right) \tag{A7}$$

$$M_{32} = -\frac{G}{na^2}\left(\frac{\partial Y}{\partial h} + kb\frac{\dot{Y}}{n}\right) \tag{A8}$$

$$M_{33} = -\frac{h}{Gna^2}(qY - qX) \tag{A9}$$

$$M_{41} = 0 \tag{A10}$$

$$M_{42} = 0 \tag{A11}$$

$$M_{43} = \frac{KY}{2Gna^2} \tag{A12}$$

$$M_{51} = 0 \tag{A13}$$

$$M_{52} = 0 \tag{A14}$$

$$M_{53} = \frac{KX}{2Gna^2} \tag{A15}$$

$$M_{61} = \frac{1}{na^2}\left[-2X + G\left(hb\frac{\partial X}{\partial h} + kb\frac{\partial X}{\partial k}\right)\right] \tag{A16}$$

$$M_{62} = \frac{1}{na^2}\left[-2Y + G\left(hb\frac{\partial Y}{\partial h} + kb\frac{\partial Y}{\partial k}\right)\right] \tag{A17}$$

$$M_{63} = \frac{qY - pX}{Gna^2} \tag{A18}$$

$$X = a[(1-h^2b)\cos F + hkb\sin F - k] \tag{A19}$$

$$Y = a[hkb\cos F + (1-k^2b)\sin F - h] \tag{A20}$$

$$\dot{X} = \frac{a^2n}{n}[hkb\cos F - (1-h^2b)\sin F] \tag{A21}$$

$$\dot{Y} = \frac{a^2n}{r}[(1-k^2b)\cos F - hkb\sin F] \tag{A22}$$

$$G = (1-k^2-h^2)^{\frac{1}{2}} \tag{A23}$$

$$b = \frac{1}{1+G} \tag{A24}$$

$$r = a(1 - k\cos F - h\sin F) \tag{A25}$$

$$K = 1 + p^2 + q^2 \tag{A26}$$

$$n = \left(\frac{\mu}{a^3}\right)^{\frac{1}{2}} \tag{A27}$$

$$\frac{\partial X}{\partial h} = a\left[-(h\cos F - k\sin F)\left(b + \frac{h^2b^3}{1-b}\right) - \frac{a}{r}\cos F(hb - \sin F)\right] \tag{A28}$$

$$\frac{\partial X}{\partial k} = -a\left[(h\cos F - k\sin F)\frac{hkb^3}{1-b} + 1 + \frac{a}{r}\sin F(\sin F - hb)\right] \tag{A29}$$

$$\frac{\partial Y}{\partial h} = a\left[(h\cos F - k\sin F)\frac{hkb^3}{1-b} - 1 + \frac{a}{r}\cos F(kb - \cos F)\right] \tag{A30}$$

$$\frac{\partial Y}{\partial k} = a\left[(h\cos F - k\sin F)\left(b + \frac{k^2 b^3}{1-b}\right) + \frac{a}{r}\sin F(\cos F - kb)\right] \tag{A31}$$

$$\lambda = F - k\sin F + h\cos F \tag{A32}$$

References

[1]Spencer, D. B., and Culp, R. D., "An Analytical Solution Method for Near-Optimal, Continuous-Thrust Orbit Transfers," American Astronautical Society, AAS Paper 93-663, Aug. 1993.

[2]Spencer, D. B., "An Analytical Solution Method for Near-Optimal, Continuous-Thrust Orbit Transfers," Ph.D. Dissertation, Univ. of Colorado, Boulder, CO, Jan. 1994.

[3]Spencer, D. B., and Culp, R. D., "An Analytical Approach for Continuous-Thrust, LEO–GEO Transfers," AIAA Paper 94-3760, Aug. 1994.

[4]Broucke, R. A., and Cefola, P. J., "On the Equinoctial Orbit Elements," *Celestial Mechanics*, Vol. 5, 1972, pp. 303–310.

[5]Kechichian, J. A., "Equinoctial Orbit Elements: Application to Optimal Transfer Problems," AIAA Paper 90-2976, Aug. 1990.

[6]Zondervan, K. P., "Optimal Low Thrust, Three Burn Orbit Transfers with Large Plane Changes," Ph.D. Dissertation, California Inst. of Technology, Pasadena, CA, May 1983.

[7]Redding, D. C., "Optimal Low-Thrust Transfers to Geosynchronous Orbit," Rept. SUDAAR 539, Stanford Univ. Guidance and Control Lab., Stanford, CA, Sept. 1983.

F. H. Lutze
Associate Editor